J. Chem. Phys.

Probing the High-Pressure Viscosity of Hydrocarbon Mixtures using Molecular Dynamics Simulations

Nikolay D. Kondratyuk,[1,2,3] Vasily V. Pisarev,[1,3] and James P. Ewen[4]
[1)]*Joint Institute for High Temperatures of Russian Academy of Sciences, Izhorskaya st. 13 Bd.2, Moscow, Russia, 125412*
[2)]*Moscow Institute of Physics and Technology (National Research University), 9 Institutskiy per., Dolgoprudny, Moscow Region, Russia, 141701*
[3)]*Higher School of Economics, National Research University, Myasnitskaya Ulitsa, 20, Moscow, Russia, 101000*[a)]
[4)]*Department of Mechanical Engineering, Imperial College London, London SW7 2AZ, U.K.*[b)]

(Dated: 29 September 2020)

Computational predictions of the high-pressure viscosity of hydrocarbon mixtures could accelerate the development of fuels and lubricants with improved performance. In this study, we use molecular dynamics simulations to study the viscosity and density of methylcyclohexane, 1-methylnaphthalene, and their binary mixtures at 323 K and pressures of up to 500 MPa. The simulation results are in excellent agreement with previous experiments available up to 100 MPa for both pure compounds (200 MPa for 1-methylnaphthalene) as well as the binary mixtures. For 1-methylnaphthalene, the viscosity initially increases slower-than-exponential with pressure before it reaches an inflection point and then increases faster-than-exponential. The inflection point (300 MPa) occurs at a pressure slightly below the one at which 1-methylnaphthalene is expected to enter the supercooled phase (400 MPa). For methylcyclohexane, the increase in viscosity with pressure is slower-than-exponential over the entire pressure range studied. The binary mixtures show intermediate pressure-viscosity responses between the two pure cases. The applicability of equations commonly used to describe the pressure dependence of viscosity, as well as the viscosity of binary mixtures, is evaluated against the computational predictions.

I. INTRODUCTION

Accurate predictions of the shear viscosity of liquid hydrocarbons are crucial in the oil and gas industry.[1] In the downstream sector, hydrocarbon mixtures such as fuels[2] and lubricants[3] are routinely exposed to very high pressures. For example, pressures inside inside common rail diesel engines can reach 300 MPa,[2] while those inside gears, cams, and rolling bearings often exceed 1 GPa.[4] Accurate high-pressure viscosity measurements are required to understand fuel injection behaviour[2] and make reliable elastohydrodynamic lubrication film thickness and friction predictions.[5] Most previous high-pressure viscosity measurements have been conducted using either well-defined, single-component fluids or multi-component commercial fuels and lubricants, whose exact molecular composition is rarely known. Only a handful of studies have investigated the high-pressure viscosity of well-defined molecular binary mixtures.

Some of the first experimental measurements of the high-pressure viscosity of hydrocarbon binary mixtures were conducted in 1935 by Dow[6] using a falling-body viscometer. They found that, for *n*-alkane mixtures (e.g. *n*-hexane/*n*-decane), the empirical Arrhenius equation[7] for the viscosity of binary mixtures was obeyed up to pressures of 400 MPa.[6] This observation suggested that the viscosities of the *n*-alkane blends were close those expected for ideal mixtures,[8] even at very high pressure. During the 1980s, Dymond et al.[9,10] studied the viscosity of binary mixtures of normal paraffins using a falling-body viscometer up to pressures of 500 MPa. They found that the viscosity of binary mixtures of *n*-hexane + *n*-hexadecane[9] and *n*-octane + *n*-dodecane[10] deviated from that expected for ideal mixtures at high pressure. The viscosity of these mixtures was accurately described using the empirical mixing rules developed by Grunberg and Nissan[11] for non-ideal mixtures.

Only a small fraction ($< 5\%$) of the volume of a typical lubricant is made up of normal paraffins,[12] which mostly consists of *iso*-paraffins, naphthenics, and aromatics.[13] Several research groups have studied the high-pressure viscosity of binary mixtures containing these components, which are more relevant than *n*-alkanes for mineral oil-derived products. For example, Griest et al.[14] measured the high-pressure viscosity of binary blends of paraffinic, naphthenic, and aromatic hydrobarbons with 25-26 carbon atoms up to 350 MPa using a rolling-ball viscometer. They found that the viscosity of the binary mixtures was within 5 % of the pure compounds equivalent to them in molecular weight and average molecular structure. From this observation, they suggested that the viscosity of these compounds was an additive function of their constituent functional groups.[14] Dymond et al. studied the viscosity of *iso*-octane + *n*-octane[15] and toluene + *n*-hexane[16] blends using a falling-body viscometer up to 500 MPa. Tanaka et al.[17] measured the viscosity of *n*-octane + cyclohexane, *n*-dodecane + cyclohexane, and *n*-hexadecane + cyclohexane binary mixtures up to 150 MPa using a torsionally-vibrating crystal viscometer. The viscosity of all of the binary mixtures studied by Dymond et al.[15,16] and Tanaka et al.[17] could be described using the Grunberg-

[a)]Electronic mail: kondratyuk.nd@mipt.ru
[b)]Electronic mail: j.ewen@imperial.ac.uk

Nissan[11] mixing rules. Boned and co-workers have studied the high-pressure ($\leq$ 100 MPa) viscosity of a wide range of binary mixtures using a falling-body viscometer.[18–25] These mixtures have included; *n*-heptane + nonylbenzene,[18] toluene + 2,6,10,14-tetramethylpentadecane,[19] toluene + 1-methylnaphthalene,[19] toluene + heptamethylnonane,[19] *n*-heptane + methylcyclohexane,[20] *n*-heptane + 1-methylnaphthalene,[20] methylcyclohexane + 1-methyhnaphthalene,[20] 2,2,4,4,6,8,8-heptamethylnonane + tridecane,[21] 2,2,4,4,6,8,8-heptamethylnonane + 1-methylnaphthalene,[22] 2,2,4,4,6,8,8-heptamethylnonane + methylcyclohexane,[23] 2,2,4,4,6,8,8-heptamethylnonane + *cis*-decalin,[24] and methylcyclohexane + *cis*-decalin.[25] Recently, Bair and Flores-Torres[26] have studied the high-pressure viscosity of binary blends of different viscosity grades (containing different average molecular weights) of the synthetic base oil poly-alpha-olefin (PAO). They found that the Grunberg-Nissan[11] mixing rules successfully predicts the viscosity of the blends, even at very high pressure ($\leq$ 1.4 GPa).[26] However, the applicability of these mixing rules has not been tested for well-defined molecular fluids with different types of intramolecular interactions at high pressure.

In addition to experiments, molecular dynamics (MD) simulations are now frequently employed to study high-pressure viscosity of hydrocarbon fluids.[27] This has been facilitated through recent advances in force field accuracy[28] as well as MD simulation software capable of exploiting hybrid supercomputer architectures.[29–32] For example, the 10$^{\text{th}}$ and 11$^{\text{th}}$ Industrial Fluid Properties Simulation Challenges showcased the ability of molecular simulations to predict the experimental viscosity of *iso*-paraffinic (2,2,4-trimethylhexane[33]) and aromatic (1,1-diphenylethane) molecules up to 1 GPa. Several entries[34–36] achieved viscosity values in good agreement with those obtained experimentally, even at very high pressure. A common theme in the successful entries was the use of an all-atom force field, which has been shown previously to be important for accurate viscosity predictions of long-chain hydrocarbons.[28] Several other studies have used MD simulations to investigate the viscosity of hydrocarbon mixtures;[37–46] however, only a few of these have calculated viscosities at elevated pressure. In a recent study, Verma et al.[42] studied the viscosity of *n*-octane + *n*-dodecane and *n*-hexadecane + *n*-decylbenzene binary mixtures up to 200 MPa using the Green-Kubo method.[47,48] They found that the Grunberg-Nissan[11] mixing rules accurately described the mixture viscosities in the pressure range studied.[42] More recently, Pisarev and Kondratyuk[44] investigated the viscosity of liquid *n*-methane + *n*-butane + *n*-pentane ternary mixtures up to 70 MPa using the reverse nonequilibrium molecular dynamics (RNEMD) method.[49] Prentice et al.[46] studied the viscosity of a model PAO consisting of hydrogenated 1-decene trimers (80 %) and tetramers (20 %) up to 1 GPa using nonequilibrium molecular dynamics (NEMD) simulations with the SLLOD method.[50]

In this study, we use MD simulations and the Green-Kubo method[47,48] to study the high-pressure viscosity of an aromatic molecule, a cycloaliphatic molecule and several of their binary mixtures. This method is a more direct route to the low-shear (Newtonian) viscosity compared to NEMD and RNEMD.[27] We selected the methylcyclohexane (C_7H_{14}) + 1-methylnaphthalene ($C_{11}H_{10}$) binary mixture, for which density and viscosity data is available up to 100 MPa.[20] The experimental measurements were made at low shear rates, ensuring that Newtonian viscosities were measured. After verifying the selected all-atom force field up to the pressures available experimentally, we studied the viscosity of the binary mixture up to the pressures (500 MPa) commonly reached inside non-conformal lubricated contacts. We confirm the applicability of expressions commonly used to describe the pressure-viscosity response of lubricants. We also show that the Grunberg-Nissan[11] mixing rules can describe the mixture viscosity of the mixtures over the entire pressure range studied.

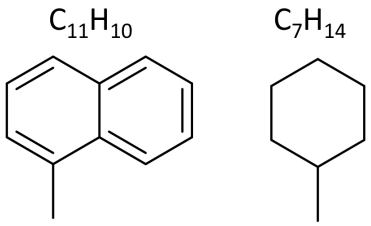

FIG. 1. Molecular structures of the studied hydrocarbons: 1-methylnaphthalene ($C_{11}H_{10}$) and methylcyclohexane (C_7H_{14}).

II. METHODOLOGY

The molecular structures of C_7H_{14} and $C_{11}H_{10}$ are shown in Fig. 1. They are representative of the low-molecular-weight naphthenic (C_7H_{14}) and aromatic ($C_{11}H_{10}$) components of diesel fuels (C_6-C_{21}[51]), and lubricant base oils (C_{10}-C_{40}[12]). Baylaucq et al.[20] have measured the density and viscosity of C_7H_{14}, $C_{11}H_{10}$, and several binary mixtures up to 100 MPa (T = 303-343 K) using a resonance densiometer and a falling-body viscometer. Data was obtained for mole fractions of C_7H_{14}, x_a = 0.000, 0.125, 0.250, 0.375, 0.500, 0.625, 0.7500, 0.875, and 1.000.[20] The viscosities of the individual components have also been reported up to higher pressures. For example, Caudwell et al.[52] measured the density and viscosity of $C_{11}H_{10}$ up to 200 MPa (T = 298-473 K) using a vibrating-wire viscometer. C_7H_{14} was one of the fluids selected by Bridgman[53] in his seminal studies on high-pressure viscosity; he measured its viscosity up to pressures exceeding 1 GPa (T = 303-348 K) using a falling-body viscometer. Jonas et al.[54] also measured the density and viscosity of C_7H_{14} up to 500 MPa (T = 203-298 K) using a rolling-ball viscometer.

The pressures inside common rail diesel engines can reach 300 MPa,[2] while those inside many lubricated engineering components often exceed 1 GPa.[4] The viscosity becomes more difficult to resolve at higher pressures in MD simulations due to the longer rotational relaxation times of the molecules.[55] In the Green-Kubo method,[47,48] this increases the integration time required, which is undesirable due to noise accumulation.[56] As a result, this approach is most suited to calculating systems with viscosities up to approxi-

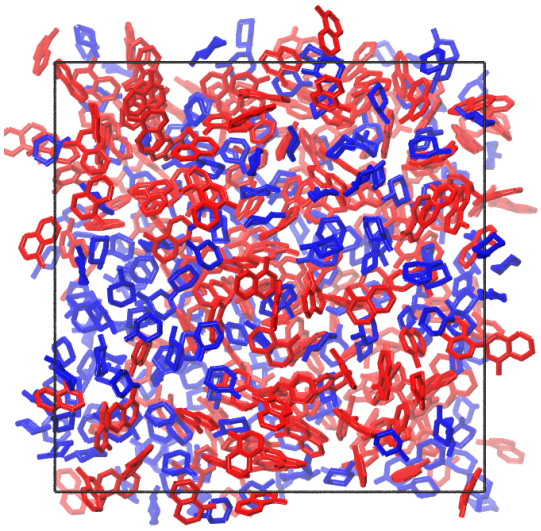

FIG. 2. A snapshot of the simulation cell containing an equimolar mixture of C_7H_{14} (blue) + $C_{11}H_{10}$ (red) during an NVT simulation at 323 K and 0.1 MPa. Hydrogen atoms and double bonds not shown. Visualized with VMD.[60]

mately 50 mPa·s.[57] For systems with higher viscosities, less direct methods, such as NEMD[27] have been successfully employed.[34,46,58] As a reasonable compromise, we studied the viscosity of the pure systems and binary mixtures up to 500 MPa in the current MD simulations. We selected an intermediate temperature (T = 323 K) from the experiments conducted by Baylaucq et al.[20] This is within the range of operating temperatures for fuels[2] and lubricants.[59]

MD simulations were performed using the Large-Scale Atomic/Molecular Massively Parallel simulator (LAMMPS) software[29] with graphic processing unit (GPU)-acceleration.[30,31] The MD simulations required significant computational resources and were performed on state-of-art hybrid supercomputers.[32] The condensed-phase optimised molecular potentials for atomistic simulation studies (COMPASS) force field,[61] with parameters obtained from *ab-initio* data, was used throughout. COMPASS is a Class II force field, the bonds and angles are described by the non-harmonic functions, and all of the intramolecular interactions exchange energy *via* cross terms.[61] In the COMPASS force field, the van der Waals interactions are represented by a 9-6 potential, rather than the conventional 12-6 Lennard-Jones form.[61] The unphysically divergent power-law repulsion causes the 12-6 form to fail at high pressure.[62] It has recently been demonstrated that COMPASS accurately predicts the high-pressure viscosity ($p < 1$ GPa) of small *iso*-paraffinic (2,2,4-trimethylpentane and 2,2,4-trimethylhexane)[35,63] and aromatic (1,1-diphenylethane)[63] hydrocarbons. The COMPASS force field, and its derivatives (such as the TEAM force field[36]) have also been used in recent high-throughput MD simulations to screen the viscosity of alkanes[64] and other organic molecules.[65] In this study, the cutoff radius for the 9-6 interactions was 12 Å, while long-range Coulomb interactions were calculated using the particle-particle, particle-mesh (PPPM) algorithm[66] with a relative error in the forces of 10^{-4}. The reversible REference System Propagator Algorithm (rRESPA) was used with a time step of 2 fs for the 9-6 and Coulomb interactions, 0.25 fs for the bonds and angles, and 1 fs for the dihedrals and impropers.[67]

The initial configurations were prepared as .car and .mdf files and then transferred to LAMMPS using the *msi2lmp* tool. The initial system for each simulation is a gas (density ≈ 0.1 g cm^{-3}) of approximately 500 randomly orientated molecules in an orthogonal simulation cell. Periodic boundary conditions were used in all three Cartesian directions. Systems with mole fractions of C_7H_{14} in $C_{11}H_{10}$, $x_a = 0.00$, 0.25, 0.50, 0.750, and 1.00, were constructed. Since the shear viscosity is not system-size dependent (above a characteristic size[68]) we use a similar number of molecules for all of the systems.

First, the systems were energy minimised using the conjugate gradient method. Next, volume of the systems was decreased over 1 ns to densities that are close to the experimental values[20] at the target temperature (323 K) and ambient pressure (0.1 MPa).[58] After the compression simulations, the systems were equilibrated in the canonical ensemble (NVT) for 1 ns. A snapshot of an equilibrated system containing an equimolar mixture ($x_a = 0.5$) of $C_7H_{14} + C_{11}H_{10}$ at 323 K and 0.1 MPa is shown in Figure 2. Each subsequent density point was obtained *via* compression for 100 ps and equilibration for a further 1 ns in the NVT ensemble at 323 K. The pressures in the NVT simulations at ambient densities are within the 0.1-1 MPa range, while the pressures at higher density have standard errors of about 3 MPa. The temperature was controlled using the Nosé-Hoover thermostat[69,70] with a damping coefficient of 1 ps. The total linear momentum was zeroed and tail corrections were applied to the energy and pressure during the simulations.[61]

We then used the Green-Kubo method[47,48] to calculate the shear viscosity, η, of the pure components and binary mixtures at zero shear rate:

$$\eta_{\alpha\beta} = \lim_{t' \to \infty} \frac{V}{k_B T} \int_0^{t'} C_\sigma(t) dt, \tag{1}$$

where t' is the integration time, V is the volume, k_B is the Boltzmann constant, T is temperature, and $C_\sigma(t)$ is the shear stress, $\sigma_{\alpha\beta}$, autocorrelation function (SACF):

$$C_\sigma(t) = \langle \sigma_{\alpha\beta}(0) \sigma_{\alpha\beta}(t) \rangle, \tag{2}$$

where the angle bracket indicates the ensemble average. In high-viscosity systems, achieving convergence of the SACF integrals can be challenging.[57] To improve convergence, we used the time decomposition method (TDM) proposed by Zhang et al.[56] Here, the Green-Kubo relation[47,48] is applied to multiple independent, short MD trajectories and the averaged running integral is used to calculate the viscosity.[56] The standard deviation in the individual running integrals is calculated

and fitted to a power-law function, which is used as a weighting function for the fitting of a double-exponential function to the averaged running integral.[56] The standard deviation is also used to determine the time range over which the running integral should be fitted.[56] For pressures below 200 MPa, SACFs were obtained by averaging over 20 independent 2 ns trajectories in the canonical (NVT) ensemble. At higher pressures, up to 70 NVT trajectories of at least 4 ns were required to obtain converged values of the shear viscosity.

The melting point of $C_{11}H_{10}$ is 242 K at atmospheric pressure and its predicted freezing pressure is expected to be approximately 400 MPa at 323 K. This estimation was made using the Simon equation[71] with parameters derived from experiments between 293-363 K and pressures up to 284 MPa.[72] Nucleation is a rare event and complex molecules do not often crystallize spontaneously on MD simulation time scales.[46] Therefore, at the highest pressures studied here ($P \geq$ 400 MPa), $C_{11}H_{10}$ is expected to be in the supercooled phase, which occurs when the liquid is cooled or pressurized rapidly enough to avoid crystallization below its melting point.[73] The melting point of C_7H_{14} is 147 K at atmospheric pressure[74] and experiments by Bridgman[53] suggested that its freezing pressure is approximately 900 MPa at 303 K. Thus, C_7H_{14} is expected to remain in the liquid phase under all of the conditions studied here. Most of the mixtures are expected to remain in the liquid phase, although those containing a high mole fraction $C_{11}H_{10}$ could enter the supercooled phase at the highest pressures studied.

III. RESULTS AND DISCUSSION

The pressure-dependence of the density for $C_{11}H_{10}$, C_7H_{14}, and the three $C_{11}H_{10}$ + C_7H_{14} binary mixtures is shown in Figure 3. For pure $C_{11}H_{10}$ ($x_a = 0.0$), the density is the same as that measured experimentally[20] within the uncertainty of the methods for all of the pressures considered. For pure C_7H_{14} ($x_a = 1.0$), the density from the MD simulations is slightly underestimated (by ≤ 2 %) compared to experiment.[20] A similar density under-prediction (≈ 1 %) has previously been reported for cyclohexane under ambient conditions using the COMPASS force field.[61] The density under-prediction of C_7H_{14} is of a similar magnitude at all of the pressures investigated here, indicating that the pressure-dependence of the density is accurately represented. For the binary mixtures, the density under-prediction compared to experiment[20] increases (from 0-2 %) with increasing mole fraction of C_7H_{14} in $C_{11}H_{10}$.

The pressure-density response of hydrocarbons is commonly described using the Tait equation:[75]

$$\frac{\rho - \rho_0}{\rho} = A \log\left(\frac{B+P}{B+P_0}\right), \qquad (3)$$

where A and B are tunable parameters, ρ is the density at pressure P, ρ_0 is density at pressure P_0, which is close to ambient. The parameters used for the fits to the Tait equation[75] in Figure 3 are given in Table I. For all of the systems and conditions studied, the Tait equation provides an excellent estimation of the density from the MD simulations, as demonstrated by the small average absolute deviations (AADs).

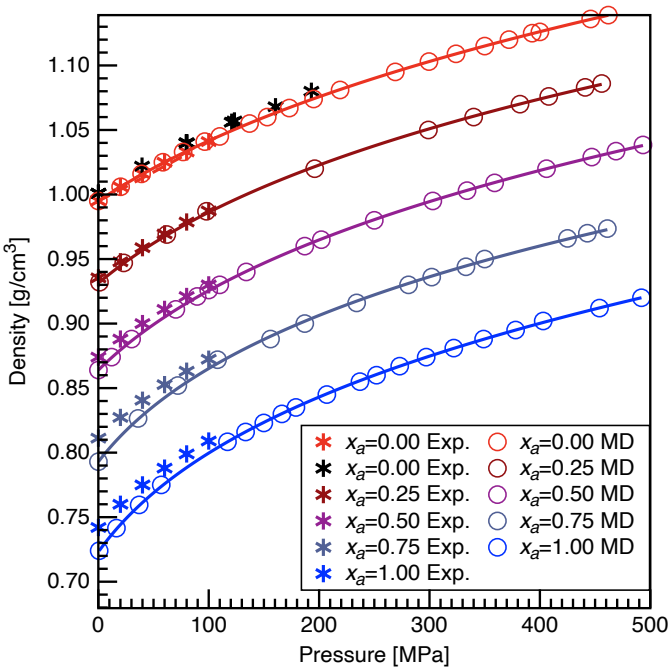

FIG. 3. The dependence of density on pressure for the pure compounds and binary mixtures at T = 323 K. Experimental data from Baylaucq et al.[20] and Caudwell et al.[52] (black). The solid lines are fits to the MD data using Equation 3 (Tait[75]). The error bars are smaller than the symbol size.

x_a	ρ_0 / g·cm^{-3}	A	B / MPa	AAD
0.00	0.995	0.0952	166.7	0.03%
0.25	0.932	0.0869	112.5	0.26%
0.50	0.864	0.0908	92.5	0.77%
0.75	0.793	0.0862	61.2	1.43%
1.00	0.724	0.0946	56.9	1.76%

TABLE I. Parameters with the relative standard errors used in the fits to Equation 3 (Tait[75]) for the MD data in Figure 3 for different mole fractions of C_7H_{14}, x_a, in $C_{11}H_{10}$. The average absolute deviations (AADs) are between the experiment and the Tait approximations of MD data.

In the MD simulations, the viscosity was calculated from the Green-Kubo[47,48] integrals. Figure 4 shows some representative examples of the convergence of the viscosity using different integration times in Equation 2. Each colored line corresponds to a mean value obtained from 20-70 independent MD trajectories of at least 1 ns. The black dotted lines are approximations from the TDM.[56]

High-viscosity systems require longer integration times, which leads to increased uncertainty due to the accumulation of noise.[56] Figure 4 shows that, for systems with low viscosity (e.g. x_a = 0.00 at 100 MPa), the Green-Kubo[47,48] integrals converge without using the TDM. For systems with higher viscosity (e.g. x_a = 0.25 at 456 MPa), the TDM[56] is required in order to obtain converged viscosity values. It is

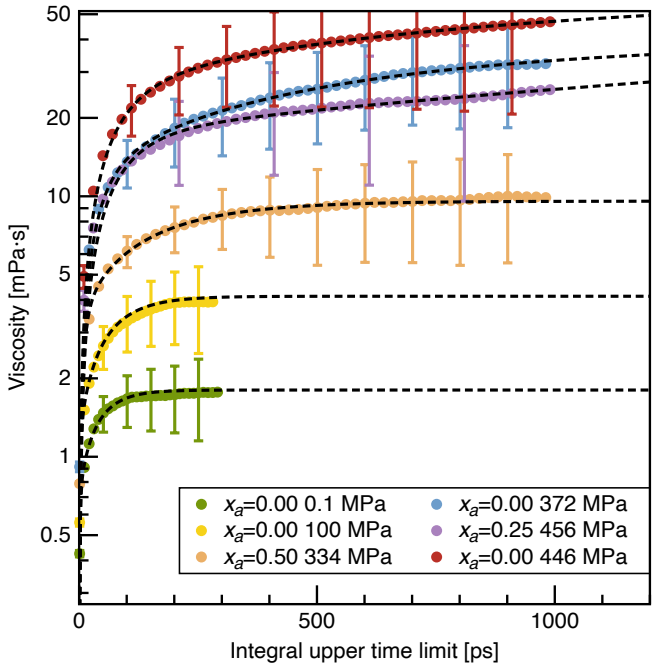

FIG. 4. Representative examples of the convergence of the viscosity, η, from the Green-Kubo[47,48] integrals using different integration upper time limits, t' (Equation 2). Black dotted lines are estimates from the TDM.[56] Error bars represent one standard deviation between the independent trajectories.

noteworthy that the highest viscosity values obtained in Figure 4 are above those usually deemed practical with the Green-Kubo[47,48] method ($\leq$ 50 mPa·s).[57]

Figure 5 shows the pressure dependence of viscosity for $C_{11}H_{10}$, C_7H_{14}, and the three $C_{11}H_{10}$ + C_7H_{14} binary mixtures. For all of the studied systems, there is excellent agreement between the experimental viscosity data from Baylaucq et al.[20] ($P \leq 100$ MPa) and the current MD simulations. For $C_{11}H_{10}$, there is also quantitative agreement between the MD simulations and the experimental data by Caudwell et al.[52] ($P \leq 200$ MPa) within the uncertainty of the methods. Below 100 MPa, the viscosity increases approximately exponentially with increasing pressure for both the pure fluids and the binary mixtures. Comparing the two pure fluids at low pressure, C_7H_{14} has a lower viscosity (η_0 in Table 5) than $C_{11}H_{10}$, but a slightly higher pressure-viscosity coefficient (α_0 in Table 5). The higher viscosity of $C_{11}H_{10}$ compared to C_7H_{14} can be explained by the larger size of the molecule (leading to more van der Waals interactions) and the presence of aromatic-aromatic interactions in $C_{11}H_{10}$.[14,76] Previous experiments have shown that naphthenic base oils (C_7H_{14}) generally have higher pressure-viscosity coefficients compared to aromatic base oils ($C_{11}H_{10}$).[77] The strong pressure-dependency of viscosity in naphthenic base oils is generally attributed to the large steric bulk of cycloaliphatic groups, which begin to interlock at moderate pressure.[78]

When $P > 100$ MPa, the pressure-viscosity response of C_7H_{14} becomes slower-than exponential, as is commonly observed for relatively low-viscosity lubricants at moderate pressure.[79] This type of pressure-viscosity response is commonly represented using the Roelands[80] or McEwen[81] equations.[79] In the McEwen equation:[81]

$$\eta = \eta_0 \left(1 + \frac{\alpha_0 P}{q-1}\right)^q, \tag{4}$$

where η_0 is the low-shear viscosity at zero pressure, α_0 is the pressure-viscosity coefficient, and q is the McEwen exponent. This is equivalent to the Tait pressure–viscosity equation[75] for low (ambient) reference pressures.[79] The blue line in Figure 5 shows a fit to the McEwen[81] equation for C_7H_{14}, the fitting parameters are provided in Table II.

When $P < 300$ MPa, the viscosity of $C_{11}H_{10}$ increases slower-than exponentially with pressure. At higher pressure, the viscosity reaches an inflection point (triangles in Fig. 5), manifesting the transition to faster-than-exponential growth of viscosity with pressure. The pressure at the inflection point ($P \approx 300$ MPa) is slightly below to the freezing pressure ($P \approx 400$ MPa) predicted using the Simon equation[71] for $C_{11}H_{10}$ at 323 K.[72] We observe a pronounced faster-than-exponential viscosity growth above the freezing pressure, where $C_{11}H_{10}$ is expected to be in the supercooled liquid phase in the MD simulations.[46] This observation suggests that a pressure-induced glass transition[58] will occur for $C_{11}H_{10}$ at higher pressures. The McEwen equation[81] cannot reproduce the faster-than-exponential viscosity increase observed in the high-pressure region for $C_{11}H_{10}$;[79] however, this can be described using the Paluch equation.[82] The Paluch equation[82] suggests the existence of a finite pressure, p_∞, at which relaxation times diverge at a given temperature. It is analogous to the temperature where the viscosity diverges, T_0, in the Vogel-Fulcher-Tammann (VFT) equation.[73] However, the Paluch equation[82] cannot describe the slower-than-exponential viscosity increase with pressure that is observed in the low-pressure region.[5]

The type of pressure-viscosity response observed for $C_{11}H_{10}$ in Figure 5 (containing an inflection point) was first observed in 1925 by Bridgman for a wide range of fluids.[83] This response has since been reported for many relatively high-viscosity lubricants at elevated pressure.[5,26,84] Recently, Bair[85] developed a hybrid model to describe this type of pressure-viscosity response by combining the McEwen[81] and Paluch[82] equations:

$$\eta = \eta_0 \left(1 + \frac{\alpha_0 P}{q-1}\right)^q \exp\left(\frac{C_F P}{P_\infty - P}\right), \tag{5}$$

where C_F is the fragility parameter, and P_∞ is the divergence pressure proposed by Paluch.[82] The hybrid model has been used to describe the high-pressure viscosity of lubricants from both experiments[5,26,84] and MD simulations.[34] The red line in Figure 5 shows a fit to the hybrid model[85] for $C_{11}H_{10}$, with parameters given in Table II. These results shows that the COMPASS force field[61] is capable of reproducing the faster-than-exponential viscosity increase with pressure for aromatic molecules ($C_{11}H_{10}$). Although COMPASS

accurately represented the experimental viscosity of an *iso*-paraffin (2,2,4-trimethylhexane[33]) up to 500 MPa, it was not able to reproduce the inflection point at higher pressure.[35] In Figure 5, no inflection point is observed in the pressure-viscosity response of C_7H_{14} at 323 K and pressures of up to 500 MPa. This observation is consistent with previous experiments that have measured the high-pressure viscosity of C_7H_{14} by Bridgman[53] ($P \leq 1$ GPa, T = 303 K) and Jonas et al.[54] ($P \leq 500$ MPa, T = 203-298 K).

For the binary mixture containing a higher mole fraction of C_7H_{14} (x_a = 0.75), the pressure-viscosity response is very similar to pure C_7H_{14}, so the data is fit with Equation 4 (McEwen[81]). For the equimolar mixture (x_a = 0.50) and the mixture containing a higher mole fraction of $C_{11}H_{10}$ (x_a = 0.25), the viscosity shows an inflection point and increases faster-than-exponentially with pressure. The pressure-viscosity response of these systems is therefore fit with Equation 5 (hybrid[85]). The open triangles in Figure 5 show that the inflection point moves to higher pressure with increasing mole fraction of C_7H_{14}. The parameters used for the pressure-viscosity fits in Figure 5 are shown in Table II. As noted in previous studies,[34] there are substantial uncertainties in the fit values due to the large number of correlated parameters. The AADs are of a similar magnitude to those obtained from fits of the hybrid model to experimental high-pressure viscosity data for other fluids.[5]

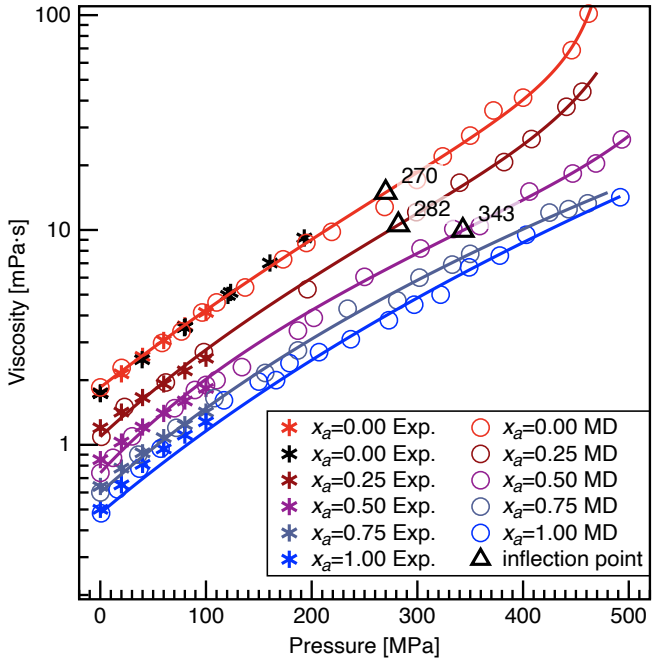

FIG. 5. The dependence of viscosity on pressure for the pure compounds and binary mixtures at T = 323 K. Experimental data from Baylaucq et al.[20] and Caudwell et al.[52] (black). The solid lines are fits to the MD data using Equation 4 (x_a = 0.75-1.00) or Equation 5 (x_a = 0.00-0.50). Error bars from the TDM method[56] are smaller than the symbol size. The inflection points of $\log \eta(p)$ dependencies according to fit (5) are shown via open triangles (x_a = 0.00-0.50) with the corresponding pressure values.

x_a	η_0 / mPa.s	α_0 / GPa^{-1}	q	C_F	p_∞ / GPa	AAD
0.00	1.85	7.38	7.11	7.08	0.50	4.2%
0.25	1.09	7.24	3.44	17.9	0.56	3.2%
0.50	0.74	7.00	2.41	18.0	0.65	6.1%
0.75	0.60	7.66	4.19	-	-	3.8%
1.00	0.48	7.82	5.44	-	-	8.0%

TABLE II. Parameters used in the fits to Equation 4 (x_a = 0.75-1.00) Equation 5 (x_a = 0.00-0.50) for the MD data in Figure 5 for different mole fractions, x_a, of C_7H_{14} in $C_{11}H_{10}$. AADs are between the fits and the MD data.

We also studied the change in viscosity with mole fraction of C_7H_{14}, x_a, at different pressures. The results are fitted with two viscosity mixing rules. Arrhenius[7] proposed the following expression to describe the viscosity of ideal binary mixtures, η_{ab}:

$$\log(\eta_{ab}) = x_a \log(\eta_a) + x_b \log(\eta_b), \tag{6}$$

where x_a and η_a are the are the mole fraction and the viscosity of component a (C_7H_{14}), and x_b and η_b are the are the mole fraction and the viscosity of component b ($C_{11}H_{10}$). Grunberg and Nissan[11] proposed a minor modification to account for non-ideality:

$$\log(\eta_{ab}) = x_a \log(\eta_a) + x_b \log(\eta_b) + x_a x_b G, \tag{7}$$

where G is a characteristic constant of the system. The Grunberg-Nissan equation successfully describes the high-pressure viscosity of many liquid hydrocarbon mixtures ranging from short n-alkanes[9,10] to commercial PAO base oils.[26] In these previous studies, the G parameter was found to be composition and pressure dependent, but was practically temperature independent for n-alkane[9,16] and other hydrocarbon[15,16] binary mixtures.

Figure 6 shows the change in logarithmic viscosity with mole fraction of C_7H_{14}, x_a, in $C_{11}H_{10}$ at different pressures. The pressures in the NVT MD simulations are not at exactly the same as those used in the experiments. Therefore, we obtained the viscosity values in Figure 6 from Figure 5 using the intercept of the pressure-viscosity fits with vertical lines at each target pressure.[34]

It is clear from Figure 6 that the viscosity of the mixtures is lower than the Arrhenius[7] predictions (Equation 6) for an ideal mixture. Negative deviations from ideality have previously been reported for the viscosity of a similar binary mixture (benzene + cyclohexane);[40] they are indicative of weak intermolecular interactions between the C_7H_{14} and $C_{11}H_{10}$ molecules. The viscosity of the equimolar mixtures is closer to the low-viscosity component (C_7H_{14}) than the high-viscosity component ($C_{11}H_{10}$), suggesting that the presence of C_7H_{14} molecules disrupts the aromatic-aromatic interactions between the $C_{11}H_{10}$ molecules.[76]

The Grunberg-Nissan[11] mixing rules (Equation 7) accurately describe the viscosity of the mixtures over the entire pressure range studied. The G parameter in the Grunberg-Nissan[11] mixing rules gives an indication as to the deviation

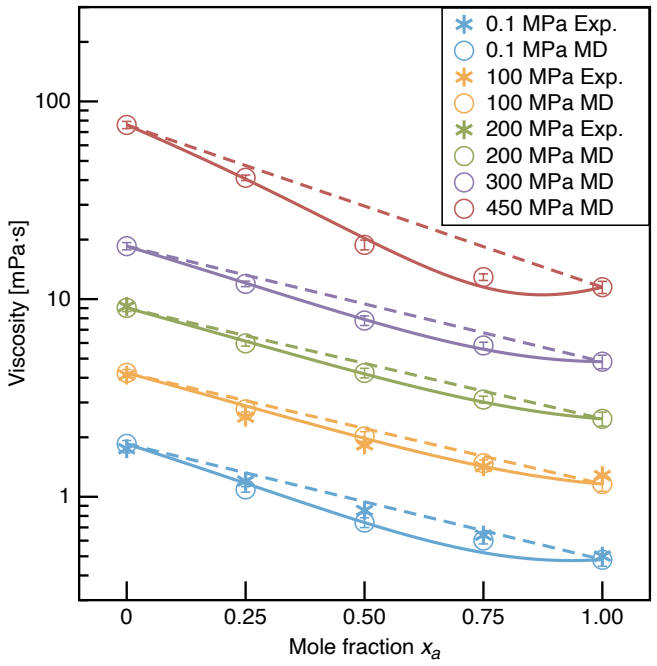

FIG. 6. The change in logarithmic viscosity with mole fraction of C_7H_{14}, x_a, in $C_{11}H_{10}$ at different pressures (T = 323 K). Experimental data from Baylaucq et al.[20] and Caudwell et al.[52] (black). The dotted lines are fits to MD η values for x_a = 0 and x_a = 1 using Equation 6 (Arrhenius[7]). The solid lines are fits to the MD data at all values of x_a using Equation 7 (Grunberg-Nissan[11]). Error bars represent the AADs from the fits in Table II.

P / MPa	η_a / mPa·s	η_b / mPa·s	G	AAD
0.1	1.85	0.48	-0.81	4.4%
100	4.23	1.16	-0.96	2.0%
200	9.03	2.48	-2.20	1.3%
300	18.53	4.82	-6.27	1.3%
450	76.05	11.48	-36.9	4.3%

TABLE III. Parameters used in the fits to Equation 6 and Equation 7 to the MD data in Figure 6. AADs are between the fits to Equation 7 and the MD data.

from ideality for the mixtures. Note that, as in previous studies of PAO mixtures,[26] a single G value was found to be sufficient to describe the viscosity of all of the mixtures at a given pressure. Compared to the MD simulations, the Grunberg-Nissan[11] mixing rule slightly overestimates the viscosity of mixtures with higher mole fraction of $C_{11}H_{10}$, and underestimates the viscosity of mixtures with higher mole fraction of C_7H_{14}. For the fits of Equation 7 to the MD data in Figure 6, the G parameter decreases roughly exponentially with pressure, as shown in Table III. A linear decrease in G with increasing pressure has been observed in previous experiments using *n*-octane + *iso*-octane binary mixtures.[15] The more rapid decrease in G with increasing pressure observed here can be explained by the fact that, at high pressure, the viscosity increases faster-than-exponential with pressure for one of the mixture components ($C_{11}H_{10}$), and slower-than-exponential for the other (C_7H_{14}).

IV. CONCLUSIONS

In this study, we use GPU-accelerated MD simulations to study the viscosity and density of the C_7H_{14} + $C_{11}H_{10}$ binary mixture at 323 K and pressures of up to 500 MPa. For the pure compounds and binary mixtures, the MD simulation results are in excellent agreement with previous experiments available up to 100 MPa. For $C_{11}H_{10}$, the simulation results are also in quantitative agreement with experimental viscosity and density data available up to 200 MPa. Over the experimental pressure range, the viscosity increases approximately exponentially with pressure for both the pure fluids and the mixtures. Comparing the low-pressure behaviour of the two fluids, C_7H_{14} has a lower viscosity than $C_{11}H_{10}$, but a slightly higher pressure-viscosity coefficient. For C_7H_{14}, the increase in viscosity with pressure becomes slower-than-exponential above 100 MPa. This type of pressure-viscosity response is accurately reproduced using the McEwen equation.[81] The pressure-viscosity response of $C_{11}H_{10}$ reaches an inflection point at around 300 MPa and then shows a faster-than-exponential increase. This type of pressure-viscosity response is described accurately using the hybrid model recently developed by Bair.[85] The onset of the faster-than-exponential increase in viscosity is slightly below the pressure at which $C_{11}H_{10}$ is expected to enter the supercooled phase at the studied temperature (400 MPa). The mixtures show intermediate pressure-viscosity responses between the two pure components. In the pressure range considered, the viscosity of the mixture with a higher mole fraction of $C_{11}H_{10}$ and the equimolar mixture show an inflection point, while the viscosity of the mixture with a higher mole fraction of C_7H_{14} does not. The viscosity of the mixtures can be accurately described over the whole pressure range using the Grunberg-Nissan mixing rules.[11] The Grunberg-Nissan G parameter is negative and the value decreases exponentially with increasing pressure, suggesting that the mixtures become much more non-ideal.

ACKNOWLEDGEMENTS

Molecular dynamics simulations, computation of densities and viscosities, estimation of simulation uncertainties, and data visualisation were performed by N.D.K. and V.V.P. with the financial support from the Russian Science Foundation (project no. 17-79-20391). Conceptualisation, literature review, and choice of fitting models was performed by J.P.E. with financial support from the Engineering and Physical Sciences Research Council (EPSRC) through grant EP/P030211/1. The simulations were performed on the Desmos and Fisher supercomputers of the Joint Institute for High Temperatures Russian Academy of Sciences, the supercomputer of the Moscow Institute of Physics and Technology (National Research University), and the HARISMa supercomputer of the National Research University Higher School of Economics.

DATA AVAILABILITY STATEMENT

LAMMPS data files and input scripts as well as the data that support the findings of this study are available from N.D.K. upon reasonable request.

REFERENCES

[1]E. Hendriks, G. M. Kontogeorgis, R. Dohrn, J. C. De Hemptinne, I. G. Economou, L. F. Zilnik, and V. Vesovic, "Industrial requirements for thermodynamics and transport properties," Ind. Eng. Chem. Res. **49**, 11131–11141 (2010).

[2]A. J. Rowane, V. Mahesh Babu, H. B. Rokni, J. D. Moore, M. Gavaises, M. Wensing, A. Gupta, and M. A. McHugh, "Effect of Composition, Temperature, and Pressure on the Viscosities and Densities of Three Diesel Fuels," J. Chem. Eng. Data **64**, 5529–5547 (2019).

[3]S. Bair and F. Qureshi, "Accurate measurements of pressure-viscosity behavior in lubricants," Tribol. Trans. **45**, 390–396 (2002).

[4]J. Zhang and H. Spikes, "Measurement of EHD Friction at Very High Contact Pressures," Tribol. Lett. **68**, 42 (2020).

[5]S. Bair, L. Martinie, and P. Vergne, "Classical EHL Versus Quantitative EHL: A Perspective Part II-Super-Arrhenius Piezoviscosity, an Essential Component of Elastohydrodynamic Friction Missing from Classical EHL," Tribol. Lett. **63**, 37 (2016).

[6]R. B. Dow, "The viscosity of mixtures of liquids at high pressures," J. Appl. Phys. **6**, 71–79 (1935).

[7]S. Arrhenius, "Über die Dissociation der in Wasser gelösten Stoffe," Z. Phys. Chem. **1**, 285 (1887).

[8]J. Kendall and K. P. Monroe, "The viscosity of liquids. II. The viscosity-composition curve for ideal liquid mixtures," J. Am. Chem. Soc. **39**, 1787–1802 (1917).

[9]J. H. Dymond, K. J. Young, and J. D. Isdale, "Transport properties of nonelectrolyte liquid mixtures-II. Viscosity Coefficients for the n-Hexane + n-Hexadecane System at Temperatures from 25 to 100°C at Pressures Up to the Freezing Pressure or 500 MPa," Int. J. Thermophys. **1**, 345–373 (1980).

[10]J. H. Dymond, J. Robertson, and J. D. Isdale, "Transport Properties of Nonelectrolyte Liquid Mixtures-III. Viscosity Coefficients for the n-Octane, n-Dodecane, and Equimolar Mixtures of n-Octane + n-Dodecane and n-Hexane + n-Dodecane from 25 to 100°C at Pressures Up to the Freezing Pressure or 500 MPa," Int. J. Thermodyn. **2**, 133–154 (1981).

[11]L. Grunberg and A. H. Nissan, "Mixture Law for Viscosity," Nature **164**, 799–800 (1949).

[12]J. Manheim, K. Wehde, W. T. J. Zhang, P. Vozka, M. Romanczyk, G. Kilaz, and H. I. Kenttämaa, "Identification and Quantitation of Linear Alkanes in Lubricant Base Oils by Using GCxGC/EI TOF Mass Spectrometry," J. Am. Soc. Mass Spectrom. **30**, 2670–2677 (2019).

[13]L. A. Mikeska, "Chemical Structure of Lubricating Oils," Ind. Eng. Chem. **28**, 970–984 (1936).

[14]E. M. Griest, W. Webb, and R. W. Schiessler, "Effect of pressure on viscosity of higher hydrocarbons and their mixtures," J. Chem. Phys. **29**, 711–720 (1958).

[15]J. H. Dymond, N. F. Glen, and J. D. Isdale, "Transport properties of nonelectrolyte liquid mixtures-VII. Viscosity coefficients for isooctane and for equimolar mixtures of isooctane + n-octane and isooctane + n-dodecane from 25 to 100°C at pressures up to 500 MPa or to the freezing pressure," Int. J. Thermophys. **6**, 233–250 (1985).

[16]J. H. Dymond, M. A. Awan, N. F. Glen, and J. D. Isdale, "Transport properties of nonelectrolyte liquid mixtures. VIII. Viscosity coefficients for toluene and for three mixtures of toluene + hexane from 25 to 100°C at pressures up to 500 MPa," Int. J. Thermophys. **12**, 275–287 (1991).

[17]Y. Tanaka, H. Hosokawa, H. Kubota, and T. Makita, "Viscosity and density of binary mixtures of cyclohexane with n-octane, n-dodecane, and n-hexadecane under high pressures," Int. J. Thermophys. **12**, 245–264 (1991).

[18]M. Kanti, B. Lagourette, J. Alliez, and C. Boned, "Viscosity of binary heptane-nonylbenzene as a function of pressure and temperature: application of Flory's theory," Fluid Phase Equilib. **65**, 291–304 (1991).

[19]A. Et-Tahir, C. Boned, B. Lagourette, and P. Xans, "Determination of the viscosity of various hydrocarbons and mixtures of hydrocarbons versus temperature and pressure," Int. J. Thermophys. **16**, 1309–1334 (1995).

[20]A. Baylaucq, C. Boned, P. Dauge, and B. Lagourette, "Measurements of the viscosity and density of three hydrocarbons and the three associated binary mixtures versus pressure and temperature," Int. J. Thermophys. **18**, 3–23 (1997).

[21]P. Daugé, A. Baylaucq, X. Canet, and C. Boned, "High pressure viscosity and density measurements of the binary mixture tridecane + 2,2,4,4,6,8,8-heptamethylnonane," High Press. Res. **18**, 291–296 (2000).

[22]X. Canet, P. Daugé, A. Baylaucq, C. Boned, C. K. Zéberg-Mikkelsen, S. E. Quiñones-Cisneros, and E. H. Stenby, "Density and viscosity of the 1-methylnaphthalene+2,2,4,4,6,8,8-heptamethylnonane system from 293.15 to 353.15 K at pressures up to 100 MPa," Int. J. Thermophys. **22**, 1669–1689 (2001).

[23]C. K. Zéberg-Mikkelsen, M. Barrouhou, A. Baylaucq, and C. Boned, "Measurements of the viscosity and density versus temperature and pressure for the binary system methylcyclohexane + 2,2,4,4,6,8,8-heptamethylnonane," High Temp. High Press. **34**, 591–601 (2002).

[24]M. Barrouhou, C. K. Zebérg-Mikkelsen, A. Baylaucq, and C. Boned, "High-Pressure Viscosity and Density Measurements for the Asymmetric Binary System cis-Decalin +2,2,4,4,6,8,8-Heptamethylnonane," Int. J. Thermophys. **24**, 937–952 (2003).

[25]C. K. Zéberg-Mikkelsen, M. Barrouhou, A. Baylaucq, and C. Boned, "Viscosity and Density Measurements of Binary Mixtures Composed of Methylcyclohexane + cis-Decalin Versus Temperature and Pressure," Int. J. Thermophys. **24**, 361–374 (2003).

[26]S. Bair and S. Flores-Torres, "The Viscosity of Polyalphaolefins Mixtures at High Pressure and Stress," J. Tribol. **141**, 021802 (2019).

[27]J. P. Ewen, D. M. Heyes, and D. Dini, "Advances in nonequilibrium molecular dynamics simulations of lubricants and additives," Friction **6**, 349–386 (2018).

[28]J. P. Ewen, C. Gattinoni, F. M. Thakkar, N. Morgan, H. Spikes, and D. Dini, "A Comparison of Classical Force-Fields for Molecular Dynamics Simulations of Lubricants," Materials. **9**, 651 (2016).

[29]S. Plimpton, "Fast parallel algorithms for short-range molecular-dynamics," J. Comput. Phys. **117**, 1–19 (1995).

[30]W. M. Brown, P. Wang, S. J. Plimpton, and A. N. Tharrington, "Implementing molecular dynamics on hybrid high performance computers - Short Range Forces," Comput. Phys. Commun. **182**, 898–911 (2011).

[31]W. M. Brown, A. Kohlmeyer, S. J. Plimpton, and A. N. Tharrington, "Implementing molecular dynamics on hybrid high performance computers - Particle-particle particle-mesh," Comput. Phys. Commun. **183**, 449–459 (2012).

[32]V. Stegailov, E. Dlinnova, T. Ismagilov, M. Khalilov, N. Kondratyuk, D. Makagon, A. Semenov, A. Simonov, G. Smirnov, and A. Timofeev, "Angara interconnect makes GPU-based Desmos supercomputer an efficient tool for molecular dynamics calculations," Int. J. High Perform. Comput. Appl. **33**, 507–521 (2019).

[33]S. Bair, "The pressure dependence of viscosity for 2,2,4 trimethylhexane to 1 GPa along the 20 °C isotherm," Fluid Phase Equilib. **488**, 9–12 (2019).

[34]M. A. Galvani Cunha and M. O. Robbins, "Determination of pressure-viscosity relation of 2,2,4-trimethylhexane by all-atom molecular dynamics simulation," Fluid Phase Equilib. **495**, 28–32 (2019).

[35]N. D. Kondratyuk and V. V. Pisarev, "Calculation of viscosities of branched alkanes from 0.1 to 1000 MPa by molecular dynamics methods using COMPASS force field," Fluid Phase Equilib. **498**, 151–159 (2019).

[36]Z. Gong and H. Sun, "Pressure-viscosity relation of 2,2,4-trimethylhexane predicted using all-atom TEAM force field," Fluid Phase Equilib. **497**, 64–70 (2019).

[37]L. I. Kioupis and E. J. Maginn, "Rheology, dynamics, and structure of hydrocarbon blends: a molecular dynamics study of n-hexane/n-hexadecane mixtures," Chem. Eng. J. **74**, 129–146 (1999).

[38]M. Aquing, F. Ciotta, B. Creton, C. Fejean, A. Pina, C. Dartiguelongue, J. P. M. Trusler, R. Vignais, R. Lugo, P. Ungerer, and C. Nieto-Draghi, "Composition Analysis and Viscosity Prediction of Complex Fuel Mixtures Using a Molecular-Based Approach," Energy and Fuels **26**, 2220–2230 (2012).

[39]Z. A. Makrodimitri, A. Heller, T. M. Koller, M. H. Rausch, M. S. H. Fleys, A. N. R. Bos, G. P. Van Der Laan, A. P. Fröba, and I. G. Economou, "Vis-

cosity of heavy n-alkanes and diffusion of gases therein based on molecular dynamics simulations and empirical correlations," J. Chem. Thermodyn. **91**, 101–107 (2015).
[40]G. Guevara-Carrion, T. Janzen, Y. M. Muñoz-Muñoz, and J. Vrabec, "Mutual diffusion of binary liquid mixtures containing methanol, ethanol, acetone, benzene, cyclohexane, toluene, and carbon tetrachloride," J. Chem. Phys. **144**, 124501 (2016).
[41]B. L. Mooney, B. H. Morrow, K. Van Nostrand, D. L. Prak, P. C. Trulove, R. E. Morris, J. D. Schall, J. A. Harrison, and M. T. Knippenberg, "Elucidating the Properties of Surrogate Fuel Mixtures Using Molecular Dynamics," Energy and Fuels **30**, 784–795 (2016).
[42]A. Verma, R. Cracknell, D. Doyle, and I. Rudra, "Determination of Diesel Physical Properties at Injection Pressures and Temperatures via All-Atom Molecular Simulations," SAE Int. J. Fuels Lubr. **9**, 1–8 (2016).
[43]B. H. Morrow, S. Maskey, M. Z. Gustafson, D. J. L. Prak, and J. A. Harrison, "Impact of Molecular Structure on Properties of n-Hexadecane and Alkylbenzene Binary Mixtures," J. Phys. Chem. B **122**, 6595–6603 (2018).
[44]V. Pisarev and N. Kondratyuk, "Prediction of viscosity-density dependence of liquid methane+n-butane+n-pentane mixtures using the molecular dynamics method and empirical correlations," Fluid Phase Equilib. **501**, 112273 (2019).
[45]D. L. Prak, B. H. Morrow, J. S. Cowart, and J. A. Harrison, "Binary Mixtures of Aromatic Compounds (n-Propylbenzene, 1,3,5-Trimethylbenzene, and 1,2,4-Trimethylbenzene) with 2,2,4,6,6-Pentamethylheptane: Densities, Viscosities, Speeds of Sound, Bulk Moduli, Surface Tensions, and Flash Points at 0.1 MPa," J. Chem. Eng. Data **5**, 2625–2641 (2020).
[46]Prentice, I. J., X. Liu, O. A. Nerushev, S. Balakrishnan, C. R. Pulham, and P. J. Camp, "Experimental and simulation study of the high-pressure behavior of squalane and poly-α-olefins," J. Chem. Phys. **152**, 074504 (2020).
[47]M. S. Green, "Markoff Random Processes and the Statistical Mechanics of Time-Dependent Phenomena. II. Irreversible Processes in Fluids," J. Chem. Phys. **22**, 398–413 (1954).
[48]R. Kubo, "Statistical-Mechanical Theory of Irreversible Processes. I. General Theory and Simple Applications to Magnetic and Conduction Problems," J. Phys. Soc. Jpn. **12**, 570–586 (1957).
[49]F. Müller-Plathe, "Reversing the perturbation in nonequilibrium molecular dynamics: An easy way to calculate the shear viscosity of fluids," Phys. Rev. E **59**, 4894–4898 (1999).
[50]D. J. Evans and G. P. Morriss, "Nonlinear-response theory for steady planar Couette flow," Phys. Rev. A **30**, 1528–1530 (1984).
[51]C. J. Mueller, W. J. Cannella, T. J. Bruno, B. Bunting, H. D. Dettman, J. A. Franz, M. L. Huber, M. Natarajan, W. J. Pitz, M. A. Ratcliff, and K. Wright, "Methodology for formulating diesel surrogate fuels with accurate compositional, ignition-quality, and volatility characteristics," Energy and Fuels **26**, 3284–3303 (2012).
[52]D. R. Caudwell, J. P. M. Trusler, V. Vesovic, and W. A. Wakeham, "Viscosity and Density of Five Hydrocarbon Liquids at Pressures up to 200 MPa and Temperatures up to 473 K Viscosity and Density of Five Hydrocarbon Liquids at Pressures up to 200 MPa and Temperatures up to 473 K," J. Chem. Eng. Data **54**, 359–366 (2009).
[53]P. W. Bridgman, "The Effect of Pressure on the Viscosity of Forty-Three Pure Liquids," Proc. Am. Acad. Arts Sci. **61**, 57–99 (1926).
[54]J. Jonas, D. Hasha, and S. G. Huang, "Self-diffusion and viscosity of methylcyclohexane in the dense liquid region," J. Chem. Phys. **71**, 3996–4000 (1979).
[55]L. I. Kioupis and E. J. Maginn, "Impact of molecular architecture on the high-pressure rheology of hydrocarbon fluids," J. Phys. Chem. B **104**, 7774–7783 (2000).
[56]Y. Zhang, A. Otani, and E. J. Maginn, "Reliable Viscosity Calculation from Equilibrium Molecular Dynamics Simulations: A Time Decomposition Method," J. Chem. Theory Comput. **11**, 3537–3546 (2015).
[57]E. J. Maginn, R. A. Messerly, D. J. Carlson, D. R. Roe, and R. Elliott, "Best Practices for Computing Transport Properties 1. Self-Diffusivity and Viscosity from Equilibrium Molecular Dynamics v1," Living J. Comput. Mol. Sci. **1**, 6324 (2018).
[58]V. Jadhao and M. O. Robbins, "Probing large viscosities in glass-formers with nonequilibrium simulations," Proc. Natl. Acad. Sci. U. S. A. **114**, 7952–7957 (2017).
[59]R. Rahmani, H. Rahnejat, B. Fitzsimons, and D. Dowson, "The effect of cylinder liner operating temperature on frictional loss and engine emissions in piston ring conjunction," Appl. Energy **191**, 568–581 (2017).
[60]W. Humphrey, A. Dalke, and K. Schulten, "VMD: Visual molecular dynamics," J. Mol. Graph. Model. **14**, 33–38 (1996).
[61]H. Sun, "COMPASS: An ab initio force-field optimized for condensed-phase applications - Overview with details on alkane and benzene compounds," J. Phys. Chem. B **102**, 7338–7364 (1998).
[62]T. C. O'Connor, J. Andzelm, and M. O. Robbins, "AIREBO-M: A reactive model for hydrocarbons at extreme pressures," J. Chem. Phys. **142**, 024903 (2015).
[63]N. Kondratyuk, D. Lenev, and V. Pisarev, "Transport coefficients of model lubricants up to 400 MPa from molecular dynamics," J. Chem. Phys. **152**, 191104 (2020).
[64]P. Santak and G. Conduit, "Enhancing NEMD with automatic shear rate sampling to model viscosity and correction of systematic errors in modeling density: Application to linear and light branched alkanes," J. Chem. Phys. **153**, 014102 (2020).
[65]S. Kajita, T. Kinjo, and T. Nishi, "Autonomous molecular design by Monte-Carlo tree search and rapid evaluations using molecular dynamics simulations," Commun. Phys. **3**, 77 (2020).
[66]B. A. Luty, M. E. Davis, I. G. Tironi, and W. F. van Gunsteren, "A comparison of particle-particle, particle-mesh and Ewald methods for calculating electrostatic interactions in periodic molecular-systems," Mol. Simul. **14**, 11–20 (1994).
[67]M. Tuckerman, B. J. Berne, and G. J. Martyna, "Reversible multiple time scale molecular dynamics," J. Chem. Phys. **97**, 1990–2001 (1992).
[68]K.-S. Kim, M. H. Han, C. Kim, Z. Li, G. E. Karniadakis, and E. Kyun, "Nature of intrinsic uncertainties in equilibrium molecular dynamics estimation of shear viscosity for simple and complex fluids," J. Chem. Phys. **149**, 044510 (2018).
[69]S. Nosé, "A Molecular-Dynamics Method for Simulations in the Canonical Ensemble," Mol. Phys. **52**, 255–268 (1984).
[70]W. G. Hoover, "Canonical Dynamics: Equilibrium Phase-Space Distributions," Phys. Rev. A **31**, 1695–1697 (1985).
[71]S. E. Babb, "Parameters in the Simon Equation relating pressure and melting temperature," Rev. Mod. Phys. **35**, 400–413 (1963).
[72]C. Yokoyama, T. Ebina, and S. Takahashi, "High pressure solid-liquid equilibria and PVTx relationships for the 1-methylnaphthalene-indole system," Fluid Phase Equilib. **104**, 391–402 (1995).
[73]P. G. Debenedetti and F. H. Stillinger, "Supercooled liquids and the glass transition," Nature **410**, 259–267 (2001).
[74]C. A. Angell, J. M. Sare, and E. J. Sare, "Glass transition temperatures for simple molecular liquids and their binary solutions," J. Phys. Chem. **82**, 2622–2629 (1978).
[75]J. H. Dymond and R. Malhotra, "The Tait equation: 100 years on," Int. J. Thermophys. **9**, 941–951 (1988).
[76]D. L. Severance and W. L. Jorgensen, "Aromatic-Aromatic Interactions: Free Energy Profiles for the Benzene Dimer in Water, Chloroform, and Liquid Benzene," J. Am. Chem. Soc. **112**, 4768–4774 (1990).
[77]W. R. Jones, R. L. Johnson, W. O. Winer, and D. M. Sanborn, "Pressure-Viscosity measurements for several lubricants to 5.5 x 10^8 Newtons per square meter 8 x 10^4 PSI) and 149 °C (300 F)," ASLE Trans. **18**, 249–262 (1975).
[78]B. K. Sharma and A. J. Stipanovic, "Pressure Viscosity Coefficient of Lubricant Base Oils As Estimated by Nuclear Magnetic Resonance Spectroscopy," Ind. Eng. Chem. Res. **41**, 4889–4898 (2002).
[79]S. Bair, "Pressure-viscosity response in the inlet zone for quantitative elastohydrodynamics," Tribol. Int. **97**, 272–277 (2016).
[80]C. J. A. Roelands, J. C. Vlugter, and H. I. Waterman, "The Viscosity-Temperature-Pressure Relationship of Lubricating Oils and Its Correlation With Chemical Constitution," J. Basic Eng. **85**, 601 (1963).
[81]E. McEwen, "The Effect of Variation of Viscosity With Pressure on the Load-Carrying Capacity of the Oil Film Between Gear-Teeth," J. Inst. Pet. **38**, 646–672 (1952).
[82]M. Paluch, Z. Dendzik, and S. J. Rzoska, "Scaling of high-pressure viscosity data in low-molecular-weight glass-forming liquids," Phys. Rev. B **60**, 2979–2982 (1999).
[83]P. W. Bridgman, "The viscosity of liquids under pressure," Proc. Natl. Acad. Sci. U. S. A. **11**, 603–606 (1925).
[84]S. S. Bair, O. Andersson, F. S. Qureshi, and M. M. Schirru, "New EHL Modeling Data for the Reference Liquids Squalane and Squalane plus Poly-

isoprene," Tribol. Trans. **61**, 247–255 (2017).
[85]S. Bair, "Choosing pressure-viscosity relations," High Temp. High Press. **44**, 415–428 (2015).